



CHORUS

This is the accepted manuscript made available via CHORUS. The article has been published as:

Interferometric Spectroscopy of Scattered Light Can Quantify the Statistics of Subdiffractive Refractive-Index Fluctuations

L. Cherkezyan, I. Capoglu, H. Subramanian, J. D. Rogers, D. Damania, A. Taflove, and V. Backman

Phys. Rev. Lett. **111**, 033903 — Published 19 July 2013

DOI: [10.1103/PhysRevLett.111.033903](https://doi.org/10.1103/PhysRevLett.111.033903)

Interferometric spectroscopy of scattered light can quantify the statistics of subdiffractive refractive-index fluctuations

L. Cherkezyan, I. Capoglu, H. Subramanian, J. D. Rogers, D. Damania, A. Taflove and V. Backman*

Northwestern University, Evanston, Illinois 60208, USA

Despite major importance in physics, biology, and other sciences, optical sensing of nanoscale structures in the far-zone remains an open problem due to the fundamental diffraction limit of resolution. We establish that the expected value of spectral variance ($\tilde{\Sigma}^2$) of a far-field, diffraction-limited microscope image can quantify the refractive-index fluctuations of a label-free, weakly scattering sample at subdiffraction length scales. We report the general expression of $\tilde{\Sigma}$ for an arbitrary refractive-index distribution. For an exponential refractive-index spatial correlation, we obtain a closed-form solution of $\tilde{\Sigma}$ which is in excellent agreement with three-dimensional finite-difference time-domain solutions of Maxwell's equations. Sensing complex inhomogeneous media at the nanoscale can benefit fields from material science to medical diagnostics.

Do Maxwell's equations permit determining the nature of 3-D subdiffractive refractive-index (RI) fluctuations of a linear, label-free dielectric medium in the far-zone? Recently, by capturing high spatial-frequency evanescent waves, metamaterial-based lenses and grating-assisted tomography have achieved a resolving power no longer limited by the diffraction of light [1, 2]. However, this super-resolution is confined to the transverse plane, which limits its ability to characterize 3-D inhomogeneous media.

While various nonlinear techniques have been proposed to image subdiffractive structures in 3-D [3–5], these techniques require exogenous labeling or intrinsic fluorescence, and thus only image the spatial distribution of particular molecular species.

Currently, elastic, label-free spectroscopic microscopy techniques are emerging that characterize the endogenous properties of a medium by utilizing the spectral content of a diffraction-limited microscopic image. Examples include multiple high-precision quantitative phase microscopy techniques [6–8], which measure the longitudinal integral of RI, and hence are insensitive to longitudinal RI fluctuations. Alternatively, partial-wave spectroscopic microscopy [9], confocal light scattering and absorption spectroscopy [10], and spectral encoding of spatial frequency [11] analyze the light-scattering response of inhomogeneous materials to obtain information of their subdiffractive structure in both lateral and longitudinal dimensions. However, the reported theory behind these techniques involves strong assumptions such as one-dimensional light transport, approximation of the medium as solid spheres, or having a single length scale.

Here, we establish that the spectral signature of scattered light in a far-zone microscope image contains sufficient information to quantify the 3-D RI fluctuations of weakly scattering media at deeply subdiffractive scales. We report three-dimensional light transport theory for linear, label-free weakly scattering media with an arbitrary form of RI distribution: continuous or discrete, random or deterministic, statistically isotropic or not. We consider the expected value of spectral variance ($\tilde{\Sigma}^2$) of a

far-field, diffraction-limited image registered by a microscope with a small numerical aperture (NA) of illumination and spectrally resolved image acquisition. We show that $\tilde{\Sigma}$ quantifies RI fluctuations at nanometer length scales limited only by the signal-to-noise ratio of the system. Under the single scattering approximation, we obtain an explicit expression relating $\tilde{\Sigma}$ to the statistics of RI fluctuations inside the sample. Moreover, for the special case of an exponential form of the RI spatial correlation, we present a closed-form solution for $\tilde{\Sigma}$ and validate it via numerical simulations of an experiment based on rigorous 3-D finite-difference time-domain (FDTD) solutions of Maxwell's equations [12].

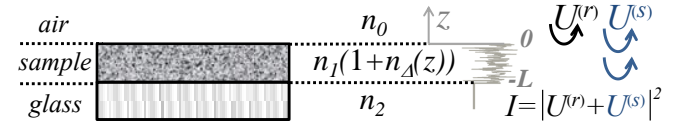


FIG. 1. Sample: RI of the middle layer is random, RIs of the top and bottom layers are constant; RI as a function of depth shown in grey. Coherent sum of $U^{(r)}$ and $U^{(s)}$ is detected. Reflection from the bottom of the substrate (glass slide) is negligible as its thickness (1mm) is much larger than the microscope's depth of field (for most setups, .5-15 μm).

Consider a spatially-varying RI object sandwiched between two semi-infinite homogeneous media (Fig. 1). The RIs of the three media are, from top to bottom: n_0 , $n_1(1 + n_\Delta(\mathbf{r}))$ (as a function of location \mathbf{r}), and n_2 . To begin with, we assume $n_1 = n_2$, approximating the case of fixed biological media on a glass slide [13, 14].

A unit amplitude plane wave with a wavevector \mathbf{k}_i is incident normally onto a weakly scattering sample. Under the Born approximation, the field inside the sample is uniform and has an amplitude $T_{01} = \frac{2n_0}{n_0 + n_1}$ (transmission Fresnel coefficient). In the far-zone, the scattering amplitude of the scalar field $U^{(s)}$, scattered from the RI fluctuations $n_\Delta(\mathbf{r})$ in the direction specified by the wavevector \mathbf{k}_o , is $f_s(\mathbf{k}_s) = T_{01} \int \frac{k^2}{2\pi} n_\Delta(\mathbf{r}') e^{-i\mathbf{k}_s \cdot \mathbf{r}'} d^3\mathbf{r}'$, where $\mathbf{k}_s = \mathbf{k}_o - \mathbf{k}_i$ is the scattering wavevector (inside the sample) [15]. The scalar-wave approximation is used here as it sufficiently describes intensity image formed

by a microscope with a moderate NA [15]. Its further justification by full-vector 3-D FDTD results is discussed below.

When the sample is imaged by an epi-illumination bright-field microscope, the back-propagating field reflected from the sample's top surface, $U^{(r)}$, returns to the image plane. Meanwhile, only the part of $U^{(s)}$ that propagates at solid angles within the NA of the objective is collected. For a microscope with magnification M , moderate NA ($k_z \approx k$), ignoring the angular dependence of the Fresnel coefficient $T_{10} = \frac{2n_1}{n_0+n_1}$, $U^{(s)}$ focused at a point (x', y') in the image plane is [16]:

$$U_{im}^{(s)}(x', y', k) = \frac{kT_{10}}{i2\pi|M|} \iint T_{kNA} f_s e^{-i(k_x x' + k_y y')} d\frac{k_x}{k} d\frac{k_y}{k} \quad (1)$$

where T_{kNA} is the microscope's pupil function - a cone in the spatial-frequency space with a radius kNA (Fig. 2a). Thus, the objective performs low-pass transverse-plane spatial frequency filtering, with the cutoff corresponding to the spatial coherence length. Substituting f_s into Eq. 1 and introducing a windowing function $T_{\mathbf{k}_s}$ that equals one at $\mathbf{k} = \mathbf{k}_s$ and zero at $\mathbf{k} \neq \mathbf{k}_s$ (Fig. 2a), $U_{im}^{(s)}$ is:

$$U_{im}^{(s)}(x', y', k) = \frac{T_{10}T_{01}}{i|M|} \int_{-\infty}^{\infty} kn_{1D}(\mathbf{r}) e^{-i2kz} dz \quad (2)$$

where \mathbf{r} is $(\frac{x'}{M}, \frac{y'}{M}, z)$ inside the sample, and n_{1D} is the $n_{\Delta}(\mathbf{r})$ convolved (\otimes) with the unitary Fourier transform (\mathcal{F}) of $T_{kNA}T_{\mathbf{k}_s}$ in the transverse plane (xy, \perp), $n_{1D}(\mathbf{r}) = \mathcal{F}_{\perp} \{T_{kNA}T_{\mathbf{k}_s}\} \otimes_{\perp} n_{\Delta}(\mathbf{r})$.

Equation 2 presents a new treatment of the Born approximation, which is here extended to include the optical imaging of a scattering object in the far-zone. Mathematically, Eq. 2 signifies that to describe a microscope-generated spectrum (a 1-D signal), the 3-D problem of light propagation can be reduced to a 1-D problem where the RI is convolved with the Airy disk in the transverse plane.

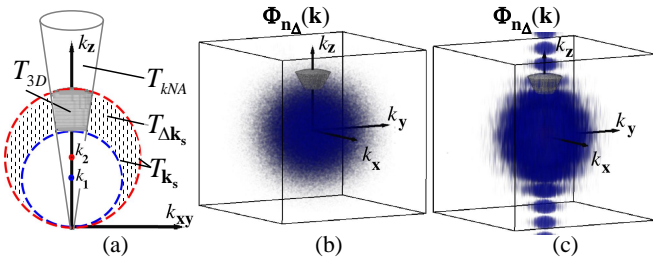


FIG. 2. Spatial-frequency space with k_z -axis antiparallel to \mathbf{k}_i . (a) Cross-section of $T_{\Delta\mathbf{k}_s}$, T_{kNA} , and their interception, T_{3D} ; (b) PSD of the RI fluctuation (blue) and T_{3D} (grey) when $l_c \ll L$; and (c) $l_c \lesssim L$.

The microscope image intensity (normalized by the image of the source), is an interferogram:

$$I(x', y', k) = \Gamma_{01}^2 - 2\Gamma\mathcal{I} \left\{ \int_{-\infty}^{+\infty} kn_{1D}(\mathbf{r}) e^{-i2kz} dz \right\} \quad (3)$$

where $\Gamma_{01} = \frac{n_0 - n_1}{n_0 + n_1}$ is Fresnel reflectance coefficient, $\Gamma = \Gamma_{01}T_{01}T_{10}$, \mathcal{I} denotes “the imaginary part of”, and n_{1D} is zero at $z \notin (-L, 0)$. Here $O(n_{\Delta}^2)$ terms are neglected.

We quantify the spatial distribution of n_{Δ} via Σ^2 - the spectral variance of the image intensity within the illumination bandwidth Δk . Since the expectation of the spectrally averaged image intensity equals Γ_{01}^2 , $\Sigma^2(x', y')$ is defined as $\Sigma^2(x', y') = \int_{\Delta k} (I(x', y', k) - \Gamma_{01}^2)^2 dk / \Delta k$. For convenience, we introduce a windowing function $T_{\Delta\mathbf{k}_s}$ that is a unity at $\mathbf{k} = \mathbf{k}_s$ for all \mathbf{k}_i with magnitudes within the Δk of the system and is zero elsewhere ($|\mathbf{k}_i|$ between k_1 and k_2 in Fig. 2a). Denoting k_c as the value of the central wavenumber of illumination bandwidth inside the sample, approximating $\Delta k \ll k_c$, applying the convolution and the Parseval's theorems (for mathematical details see the Supplemental Material), $\Sigma^2(x', y')$ equals:

$$\Sigma^2(x', y') = \frac{\Gamma^2 k_c^2}{\Delta k} \int_{-\infty}^{\infty} |\mathcal{F} \{T_{\Delta\mathbf{k}_s} T_{kNA}\} \otimes n_{\Delta}(\mathbf{r})|^2 dz \quad (4)$$

Physically, $T_{\Delta\mathbf{k}_s}$ accounts for the limited bandwidth of illumination and serves as a band-pass longitudinal spatial-frequency filter of RI distribution with its width related to the temporal coherence length, $l_{\tau} = 2\pi/\Delta k$. The interception of the two frequency filters associated with the spatial and temporal coherence, T_{kNA} and $T_{\Delta\mathbf{k}_s}$, signifies the frequency-space coherence volume centered at $k_z = 2k_c$: $T_{3D} = T_{\Delta\mathbf{k}_s} T_{kNA}$ (Fig. 2a). Given an infinite bandwidth, one could reconstruct the full 3-D RI from $I(x', y', k)$. However, since Δk and k_c are finite, Σ detects the variance of an “effective RI distribution”, i.e. of $n_{\Delta}(\mathbf{r}) \otimes \mathcal{F} \{T_{3D}\}$ (Eq. 4).

Note that $\Sigma^2(x', y')$ is random since $n_{\Delta}(\mathbf{r})$ is random. Hence, to characterize the sample statistics, we compute its expected value, denoted as $\tilde{\Sigma}^2$. Using the Wiener-Khinchine relation, we obtain $\tilde{\Sigma}^2$ from Eq. 4 as:

$$\tilde{\Sigma}^2 = \frac{\Gamma^2 k_c^2 L}{\Delta k} \int_{T_{3D}} \Phi_{n_{\Delta}}(\mathbf{k}) d^3\mathbf{k} \quad (5)$$

where $\Phi_{n_{\Delta}} = |\mathcal{F} \{n_{\Delta}(\mathbf{r})\}|^2$ is the power spectral density (PSD) of n_{Δ} .

Equation 5 establishes the general quadrature-form expression for $\tilde{\Sigma}^2$ for an arbitrary $n_{\Delta}(\mathbf{r})$. Note that while the 3-D structure of complex inhomogeneous materials cannot be described by a single measure of size or RI, the $\Phi_{n_{\Delta}}$ fully quantifies the magnitude, spatial frequency, and orientation of all RI fluctuations present within the sample. As seen from Eq. 5, $\tilde{\Sigma}^2$ measures the integral of the tail of the PSD within T_{3D} . Hence, as shown later, $\tilde{\Sigma}^2$ presents a monotonic measure of the width of the PSD. When $n_1 \neq n_2$, the expression for $\tilde{\Sigma}^2$ has a different pre-factor and a deterministic offset, specified in the Supplemental Material.

We further obtain a closed-form expression for $\tilde{\Sigma}^2$ for a special case when $n_{\Delta}(\mathbf{r})$ has an exponential form of spatial correlation with a variance $\sigma_{n_{\Delta}}$ and correlation distance l_c . Since l_c can only be defined for a random

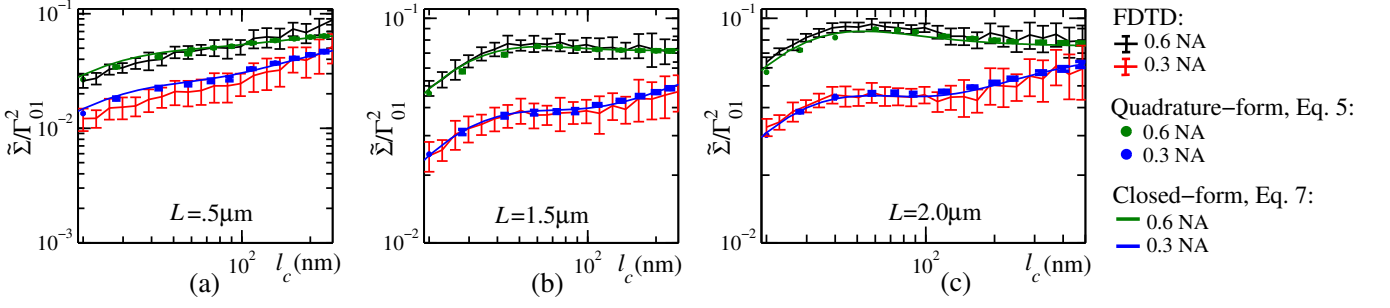


FIG. 3. $\tilde{\Sigma}$ dependence on l_c predicted by the quadrature-form (Eq. 5) and the closed-form (Eq. 7) analytical expressions for $\tilde{\Sigma}$ (circles and solid lines correspondingly), and by FDTD (solid lines with error bars representing standard deviation between 20 realizations of each statistical condition), calculated for (a) $L=0.5\mu\text{m}$, $\Delta k = 4.9\mu\text{m}^{-1}$, $k_c = 16.8\mu\text{m}^{-1}$, (b) $L=1.5\mu\text{m}$, $\Delta k = 4.9\mu\text{m}^{-1}$, $k_c = 16.8\mu\text{m}^{-1}$, and (c) $L=2.0\mu\text{m}$, $\Delta k = 11.9\mu\text{m}^{-1}$, $k_c = 18.1\mu\text{m}^{-1}$ (wavenumber values in inside the sample). Data shown normalized by Γ_{01}^2 , the image intensity in the absence of RI fluctuations inside the sample.

medium with a physical size much larger than the correlation distance, we define l_c as the correlation distance of an unbounded medium $n_{\Delta}^{\infty}(\mathbf{r})$, and the sample as a horizontal slice of $n_{\Delta}^{\infty}(\mathbf{r})$ with thickness L : $n_{\Delta}(\mathbf{r}) = T_L n_{\Delta}^{\infty}(\mathbf{r})$ where T_L is a windowing function along the z -axis with width L . The PSD of such sample is an anisotropic function of l_c and L : $\Phi_{\mathbf{n}_{\Delta}}(\mathbf{k}) = |\mathcal{F}\{T_L\} \otimes \mathcal{F}\{n_{\Delta}^{\infty}\}|^2$ (Fig. 2b,c). Alternatively, $\tilde{\Sigma}^2$ is found by independently computing the contributions from i) scattering from within the sample ($\tilde{\Sigma}_R^2$), and ii) reflectance at $z = -L$ ($\tilde{\Sigma}_L^2$):

$$\tilde{\Sigma}^2 = \tilde{\Sigma}_R^2 + \tilde{\Sigma}_L^2 \quad (6)$$

Here, $\tilde{\Sigma}_L$ is fully described by the RI contrast at the bottom surface, $\tilde{\Sigma}_L^2 = \Gamma^2 \sigma_{\perp}^2(n_{1D})/4$, where $\sigma_{\perp}^2(n_{1D})$ is the variance of the effective n_{1D} in the transverse plane (details shown in the Supplemental Material). $\tilde{\Sigma}_R$, in turn, is defined by $\Phi_{\mathbf{n}_{\Delta}^{\infty}}$, which is independent of L when $L \gtrsim l_{\tau}$. $\tilde{\Sigma}_R$ is obtained by integrating the PSD of an exponentially correlated $n_{\Delta}^{\infty}(\mathbf{r})$ according to Eq. 5. Substituting $\tilde{\Sigma}_R^2$ and $\tilde{\Sigma}_L^2$ into Eq. 6, and introducing a unitless size parameter $x = k_c l_c$, we obtain the following closed-form solution for $\tilde{\Sigma}^2$ for an exponential form of the spatial RI correlation:

$$\tilde{\Sigma}^2 = \frac{2\Gamma^2 \sigma_{n_{\Delta}}^2}{\pi} \frac{k_c L x^3 N A^2}{(1 + x^2(4 + N A^2))(1 + 4x^2)} + \Gamma^2 \sigma_{n_{\Delta}}^2 (1 - 1/\sqrt{1 + (x N A)^2})/4 \quad (7)$$

Two assumptions were made to derive Eq. 7 from Eq. 5: 1) we approximated the top and bottom surfaces of T_{3D} as planes perpendicular to the k_z axis, 2) we calculated $\tilde{\Sigma}_R$ from $\Phi_{\mathbf{n}_{\Delta}^{\infty}}$, not considering the extreme case of $L \ll l_{\tau}$. Both assumptions are not crucial from the theoretical perspective are there only to obtain a relatively simple closed-form solution of Eq. 5.

To confirm these approximations, we evaluate $\tilde{\Sigma}$ predicted by the general quadrature-form expression (Eq. 5) using Matlab computing software (MathWorks Inc). We obtain an excellent agreement between $\tilde{\Sigma}$ calculated from Eq. 5 and the closed-form expression, Eq. 7, de-

rived from it (Fig. 3). This validates the closed-form solution for $\tilde{\Sigma}$ for an exponential RI correlation.

We support the present theory by simulating a physical experiment using the rigorous 3-D FDTD solution of Maxwell's equations [17–19]. Our technique accurately synthesizes microscope images of arbitrary inhomogeneous samples under various imaging parameters, incorporating RI fluctuations as fine as 10nm. We synthesized bright-field, plane-wave epi-illumination microscope images of samples with RI distribution resembling that of biological cells: $n_1 = 1.53$ [13, 14], $n_1 \sigma_{n_{\Delta}} = 0.05$ [20]. The spatial RI correlation was set to be exponential, and the RIs of the top and bottom media were $n_0 = 1$ and $n_2 = 1.53$.

Referring to Fig. 3, the $\tilde{\Sigma}$ predicted by the present theory [either by the quadrature-form (Eq. 5) or the closed-form (Eq. 7) expressions] exhibits an excellent agreement with the FDTD-simulated experimental results over a wide range of l_c , L , spectral bandwidth and NA. The agreement is such that the theoretically-predicted $\tilde{\Sigma}$ by both Eqs. 5 and 7 lie within the standard deviation bars of the FDTD results at all points tested. While the present derivation assumes $\Delta k \ll k_c$, in fact, the closed-form analytical solution is robust for Δk that includes the full range of visible wavelengths (Fig. 3c). This match also justifies the employed scalar-wave approximation as well as that the single scattering approximation applies to RI fluctuations typical for fixed biological cells.

We next describe the l_c -dependence of $\tilde{\Sigma}$ and compare its key aspects to those of the commonly used scattering parameters: the backscattering (σ_b) and the total scattering (σ_s) cross-sections. σ_b manifests a non-monotonic dependence on l_c which makes the inverse problem ambiguous [21], while σ_s increases steeply $\propto l_c^3$ and thus is relatively insensitive to structural changes at small length scales [22]. $\tilde{\Sigma}(l_c)$, in turn, is distinguished by three important properties illustrated in Fig. 3. First, unlike σ_b , $\tilde{\Sigma}(l_c)$ can be monotonic. This property is apparent for thin samples ($L < 2\mu\text{m}$, Fig. 3a,b). For thicker samples, a smaller collection NA can be chosen so that $\tilde{\Sigma}(l_c)$ remains monotonic (e.g. NA=0.3 in Fig. 3c). Second,

as opposed to $\sigma_s(l_c)$, the sensitivity of $\tilde{\Sigma}$ to changes at smaller length scales is not obscured by changes at larger l_c . We note that the functional form of $\tilde{\Sigma}(l_c)$ for $l_c < 1/k_c$ can be roughly approximated as linear (r^2 of linear regressions for $\tilde{\Sigma}(l_c)$ presented in Fig. 3 range from .86 to .91). Finally, $\tilde{\Sigma}$ is independent of l_c for $l_c \gg 1/k_c$ and therefore $\tilde{\Sigma}(l_c)$ exhibits predominant sensitivity to sub-diffraction length scales that is only limited by the signal-to-noise ratio (SNR). The larger structures are naturally resolved in the microscope image. In addition, while the above mentioned scattering parameters are $\propto \sigma_{n_\Delta}^2$, $\tilde{\Sigma}$ is $\propto \sigma_{n_\Delta}$ (confirmed by FDTD with $r^2 = .99$, data not shown), which substantially improves the SNR.

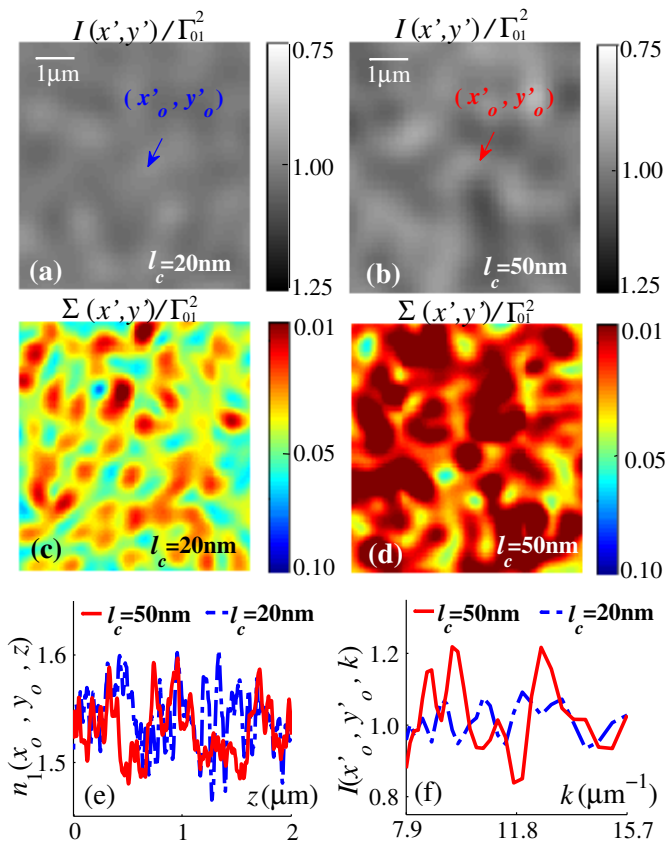


FIG. 4. 40x magnification, 0.6 NA microscope images of samples with $L = 2\mu\text{m}$ were synthesized by FDTD. Bright-field images of samples with (a) $l_c = 20\text{nm}$ and (b) $l_c = 50\text{nm}$; $\Sigma(x', y')/\Gamma_{01}^2$ obtained from the wavelength-resolved image of (c) the sample with $l_c = 20\text{nm}$ and (d) $l_c = 50\text{nm}$; (e) RI of the two samples as a function of z along central voxels (x_o, y_o) , and (f) image spectra of the corresponding pixels (x'_o, y'_o) .

Results of an FDTD-simulated experiment are shown in Fig. 4. As expected, the bright-field microscope images of samples with $l_c = 20$ and 50nm (Fig. 4a,b) are essentially indistinguishable. However, a drastic difference between the two samples is revealed in the respective $\Sigma(x', y')$ images (Fig. 4c,d; where colorbar limits match the ordinate range in Fig. 3c). Figures 4e,f illustrate that a smaller amplitude of spectral oscillations in the wavelength-resolved microscope image indicates a higher spatial frequency of the sample's RI fluctuations.

Recognizing that the experimental $n_\Delta(\mathbf{r})$ may not be exponentially correlated, one may attempt to a) use the validated approximations to obtain a closed form solution for a different functional form of the PSD from Eq. 5; b) represent the correlation function of n_Δ as a superposition of exponentials; or c) evaluate the Eq. 5 numerically (no explicit functional form of the PSD required for the latter two).

We emphasize that, while $\tilde{\Sigma}$ does not probe spatial frequencies above $2k$, the subdiffraction-scale structural alterations change the width of PSD and, therefore, the $\tilde{\Sigma}$. Thus, $\tilde{\Sigma}$ provides a monotonic *measure* for the width of the 3-D PSD of RI fluctuations with a high sensitivity to subdiffraction length scales, without actually *imaging* the 3-D RI.

We have established that despite the diffraction limit of resolution, the interferometric spectroscopy of scattered light can quantify the statistics of RI fluctuations at deeply subdiffraction length scales. We have shown that the $\tilde{\Sigma}$ obtained from an elastic, label-free, spectrally resolved far-field microscope image quantifies RI fluctuations inside weakly scattering media at length scales limited by the SNR of the detector. We have derived a closed-form analytical solution for $\tilde{\Sigma}$ that yields results that agree with numerical solutions of Maxwell's equations over a wide tested range of sample and instrument parameters. Potential applications include semiconductors, material science, biology, and medical diagnostics.

This work was supported by National Institutes of Health (NIH) grants R01CA128641, R01EB003682, and R01CA155284, and National Science Foundation (NSF) grant CBET-0937987. The FDTD simulations were made possible by a computational allocation from the Quest high-performance computing facility at Northwestern University.

* Corresponding Author: v-backman@northwestern.edu

- [1] D. Lu and Z. Liu, Nature Communications **3**, (2012).
- [2] A. Sentenac, P. C. Chaumet, and K. Belkebir, Phys. Rev. Lett. **97**, 243901 (2006).
- [3] S. W. Hell, Science **316**, 1153 (2007).
- [4] B. Huang, W. Wang, M. Bates, and X. Zhuang, Science **319**, 810 (2008).
- [5] D. W. Piston, Trends in Cell Biology **9**, 66 (1999).
- [6] G. Popescu, *Quantitative Phase Imaging of Cells and Tissues*, McGraw-Hill Biophotonics (McGraw-Hill Companies, Incorporated, 2011).
- [7] Z. Wang, L. Millet, M. Mir, H. Ding, S. Unarunotai, J. Rogers, M. U. Gillette, and G. Popescu, Opt. Express **19**, 1016 (2011).
- [8] B. Bhaduri, H. Pham, M. Mir, and G. Popescu, Opt. Lett. **37**, 1094 (2012).
- [9] H. Subramanian, P. Pradhan, Y. Liu, I. R. Capoglu, J. D. Rogers, H. K. Roy, R. E. Brand, and V. Backman, Opt. Lett. **34**, 518 (2009).
- [10] I. Itzkan, L. Qiu, H. Fang, M. M. Zaman, E. Vitkin, I. C. Ghiran, S. Salahuddin, M. Modell, C. Andersson, L. M.

- Kimerer, P. B. Cipolloni, K.-H. Lim, S. D. Freedman, I. Bigio, B. P. Sachs, E. B. Hanlon, and L. T. Perelman, *Proceedings of the National Academy of Sciences* **104**, 17255 (2007).
- [11] S. A. Alexandrov, S. Uttam, R. K. Bista, K. Staton, and Y. Liu, *Applied Physics Letters* **101**, 033702 (2012).
- [12] A. Taflove and S. C. Hagness, *Computational Electrodynamics: The Finite-Difference Time-Domain Method*, 3rd ed. (Artech House, 2005).
- [13] D. Cook, “Cellular pathology: An introduction to techniques and applications,” (Scion, 2006).
- [14] G. C. Crossmon, L. Millet, M. Mir, H. Ding, S. Unarunotai, J. Rogers, M. U. Gillette, and G. Popescu, *Stain Technology* **24**, 1016 (1949).
- [15] M. Born and E. Wolf, *Electromagnetic theory of propagation, interference and diffraction of light*, edited by Born, M. & Wolf, E. (Cambridge University Press, 1998, 1998).
- [16] J. Goodman, *Introduction To Fourier Optics*, McGraw-Hill physical and quantum electronics series (Roberts & Co., 2005) pp. 126–154.
- [17] I. R. Capoglu, “Angora: A free software package for finite-difference time-domain (FDTD) electromagnetic simulation,” (2012), date accessed: April 2012, <http://www.angorafdttd.org>.
- [18] I. R. Capoglu, J. D. Rogers, A. Taflove, and V. Backman, in *Progress in Optics*, Vol. 57, edited by E. Wolf (Elsevier, 2012) pp. 1 – 91.
- [19] I. R. Capoglu, A. Taflove, and V. Backman, (2012), *IEEE Antennas and Propagation Magazine* (in press).
- [20] J. M. Schmitt and G. Kumar, *Appl. Opt.* **37**, 2788 (1998).
- [21] A. Ishimaru, *Wave Propagation and Scattering in Random Media*, IEEE Press Series on Electromagnetic Wave Theory (Wiley, 1999).
- [22] A. J. Radosevich, J. Yi, J. D. Rogers, and V. Backman, *Opt. Lett.* **37**, 5220 (2012).